AAPS PharmSciTech 2001; 2 (1) article 4
(http://www.pharmscitech.com)

Evaluation of Preseparator Performance for the 8-Stage Nonviable Andersen Impactor

Submitted: January 1, 2001; Accepted: March 23, 2001

Vasu V. Sethuraman[1] and Anthony J. Hickey[1,2,*]

[1]Department of Biomedical Engineering
[2]School of Pharmacy, University of North Carolina at Chapel Hill; Chapel Hill, NC 27599

ABSTRACT The preseparator of an Andersen impactor with different coating treatments for a range of particle-size distributions was evaluated. Limited theoretical simulations constrained by simplifying assumptions of the airflow fields in the preseparator and upper stages of an 8-stage Andersen impactor were used to reveal low-velocity and high-pressure regions for potential deposition. These regions were then sampled in subsequent particle deposition experiments. Disodium fluorescein aerosols were sampled with different coating treatments of the preseparator floor. Particles collected at impactor stages determined particle size distributions. Stage deposition was compared between different preseparator treatments (buffer and silicon oil). Collection efficiency in the preseparator followed the pattern buffer > silicon oil > untreated. Statistical differences ($P < 0.05$) were noted in collection efficiency of large particles (45 μm-75 μm) in the preseparator. The mass median aerodynamic diameters and geometric standard deviations showed some statistical differences when different preseparator treatments for large particles were used; therefore, preseparator coating was shown to influence performance and thereby estimates of particle size by inertial impaction.

KEYWORDS: Inertial impaction, Preseparator, Wall losses, Finite element analysis

***Corresponding Author:** Anthony J. Hickey School of Pharmacy, University of North Carolina Chapel Hill, NC 27599; Telephone: 919-962-0223; Facsimile: 919-966-0197; E-mail: ahickey@unc.edu

INTRODUCTION

Understanding the flow of air that carries particles is important for aerodynamic particle size determination and lung deposition. Cascade impactors, initially described by May [1], are commonly used to study the particle dispersion on an airstream. These devices have multiple platforms, or stages, with orifices that decrease in size with each succeeding stage. Below the orifices at each stage is a collection plate. A vacuum drawn at the base of the impactor by a dedicated pump is adjusted to generate a predesignated volumetric airflow rate. Particles are drawn into the impactor on the conveying air stream. The airflow is deflected when its path is obstructed by the collection surface. Small particles with low inertia move around the surface in the air stream; however, large particles with high inertia will continue on their original paths in the air stream and impact on the collection surface. Because the orifice size decreases with succeeding stages, the linear velocity of air increases at each successive stage. The inertia of the particles increases at each stage, increasing their probability of deposition. Each collection surface can be washed and the solution assayed to determine the mass of material-originally particles-deposited on the surface. The sum of the mass of particles from each collection surface should be equivalent to the mass of particles entering the impactor; however, this is rarely the case because not all particles impact on the collection surfaces. Mass balance may not be achieved because some particles will not be recovered. These particles are commonly referred to as "wall losses" [2].

Recent advances in computer processing capacity have allowed complex flow models to be resolved by the finite element method. Finite element models of different impactors have been developed [3, 4]; however, none have dealt with the commonly used Andersen impactor [5] (Graseby Andersen, Smyrna, GA). This impactor differs from many other impactors in that each of its stages has multiple orifices. The flow of air and particles through 1 orifice may affect the flow through an adjacent orifice. In addition, none of the previous models has considered the performance of the preseparator (Figure 1) through which aerosol passes before entering the first stage in an Andersen impactor. Flow through the preseparator is a complex transition from turbulent to laminar conditions, which is not easily modeled. However, simplifying assumptions may be used to indicate the probable flow in various regions of the preseparator, which may then be used to guide experimental studies.

At a flow rate of 60 L/min, which is typically used in experimental studies with dry powder inhalers [6,7], the effective cutoff diameter for the preseparator is 8.7 μm based on calculations for evaluating impactor jets [8]. The effective cutoff diameter for the first stage (S-1) is 8.6 μm, indicating that a very small mass-only particles between 8.6 μm and 8.7 μm-should be collected on this stage. However, as previously shown [2], the preseparator efficiency is not perfect, and particles smaller than 8.6 μm do not reach the first stage. This can lead to some inaccuracies in the resulting particle size distribution; therefore, the preseparator performance is a very important issue in cascade impaction of dry powder aerosols.

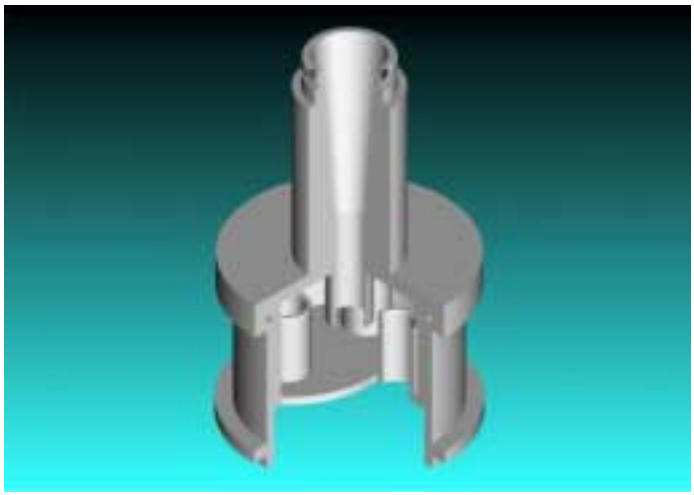

Figure 1. The preseparator of the Andersen MkII cascade impactor.

The flow of air through the impactor may be described by the Navier-Stokes partial differential equations. The simplified Navier-Stokes equations for a 2-dimensional (2-D) model, with the assumptions of constant density, viscosity, and laminar flow, are described by equations 1 and 2 for the r and z directions of a cylindrical coordinate system, where ρ is the density of the air, μ is the viscosity of the air, P is the pressure in the r or z directions, v_r and v_z are the velocities in the r and z directions, and r and z are the distances in these directions [9]:

$$\rho\left(v_r\frac{\partial v_r}{\partial r}+v_z\frac{\partial v_r}{\partial z}\right)=-\frac{\partial P}{\partial r}+\mu\left[\frac{\partial}{\partial r}\left(\frac{1}{r}\frac{\partial(rv_r)}{\partial r}\right)\right] \quad (1)$$

$$\rho\left(v_r\frac{\partial v_z}{\partial r}+v_z\frac{\partial v_z}{\partial z}\right)=-\frac{\partial P}{\partial z}+\mu\left[\frac{1}{r}\frac{\partial}{\partial r}\left(r\frac{\partial v_z}{\partial r}\right)+\frac{\partial^2 v_z}{\partial z^2}\right] \quad (2)$$

The continuity equation involved in the solution is:

$$0=\frac{1}{r}\frac{\partial(rv_r)}{\partial r}+\frac{\partial v_z}{\partial z} \quad (3)$$

Coating or using liquid in the preseparator is recommended to improve impactor efficiency by increasing deposition of particles with aerodynamic particle sizes of greater than 8.7 μm [6, 7]; however, the nature of deposition in different regions of the preseparator has not been described. This deposition affects the airflow and particle behavior in the preseparator.

Airflow through a commonly used cascade impactor, the Andersen impactor, was modeled to qualitatively define regions in which particle losses might be anticipated. In addition, experimental studies were performed to evaluate the effects of different aerosols on the preseparator efficiency after different coating procedures were used.

MATERIALS AND METHODS

Modeling

The dimensions of the impactor were determined in SI units. A representative 2-D model of the

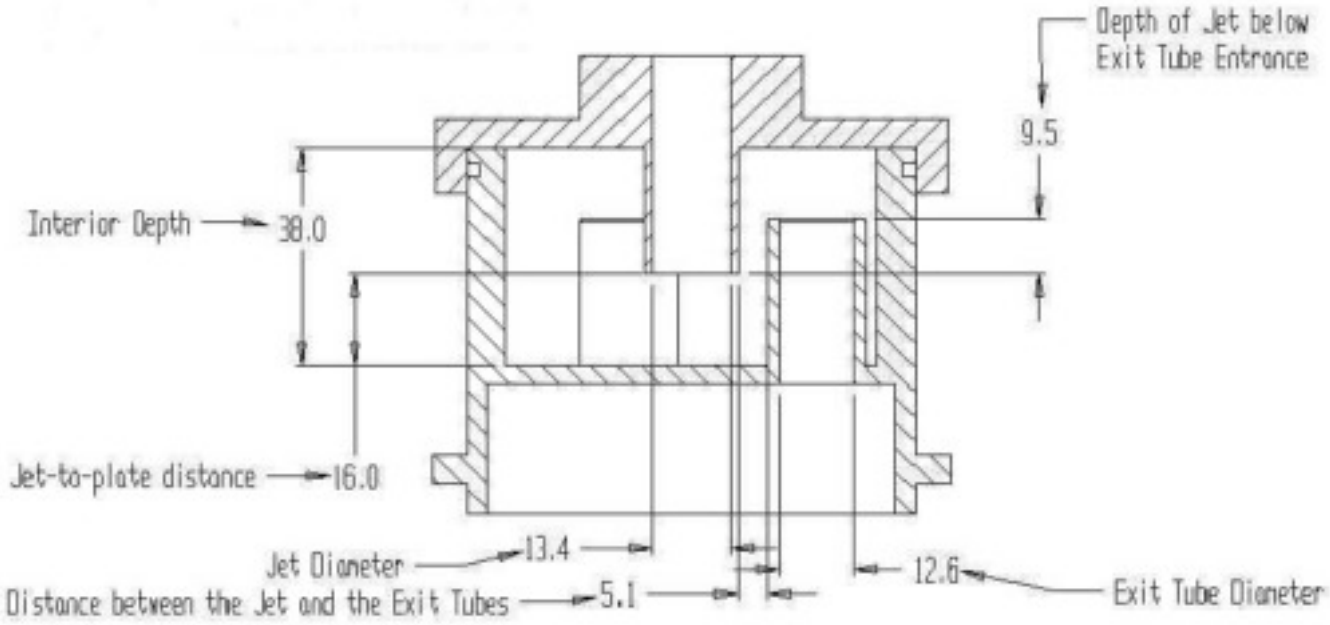

Figure 2. The preseparator with the inlet jet illustrating that the jet extends below the top of the exit tubes (all dimensions in millimeters).

preseparator and the top 3 stages, symmetric around the z-axis of the impactor, was created with FIDAP version 8.52 (Fluent Inc, Lebanon, NH). The dimensions of the preseparator and the inlet jet connection to the throat are illustrated in Figure 2. After the geometry was created, a series of assumptions were made for the system in question. The simplifying assumptions included laminar flow with constant viscosity and density. The boundary conditions were specified as zero velocity at the walls of the impactor and zero change in velocity across the side of symmetry. A flow rate of 60 L/min was used to calculate the inlet velocity based on the cross-sectional area at the inlet of the impactor. This flow rate is equivalent to the flow typically used in experimental studies with dry powder inhalers [6,7].

It is important to recognize the limitations of these models. The flow in the preseparator's inlet jet is in the turbulent regime and the flow through the exit jets may be laminar or turbulent at a flow rate of 60 L/min. However, it has been shown that the flow through the upper stages of the impactor is laminar, based on the calculated Reynolds numbers [10]. In addition, there are inaccuracies in any 2-D model of the impactor. To quantitatively describe the flow in the impactor, a 3-D model would be ideal. A more useful model might also be the preseparator in combination with the impactor stages because the flow through the preseparator is certain to affect the flow through the stages. The complexity of such a model makes it difficult to obtain a solution, however. Therefore, the geometries modeled were radial slices of the preseparator and the top 3 stages of the impactor. In addition, the flow of particles, points of finite size, and density in the flow field would be desirable in a more representative, quantitative, and predictive model of the impactor. The usefulness of the present models is to qualitatively indicate the regions of low velocity and high pressure so that experimental studies can be designed to sample deposited particles in these regions.

The elements used in the models are 4 node quadrilateral elements in the mapped mesh of the preseparator and top 3 stages (Figure 3).

Figure 3. (a) Mesh for preseparator. (b) Mesh for top 3 stages.

EXPERIMENTAL

Disodium fluorescein (DF; ICN Biomedicals, Aurora, OH) was dried to constant weight for 48 hours in a vacuum oven (Napco Model 5831, Napco, Winchester, VA) at one tenth of an atmosphere. Dried DF was micronized (jet mill, Trost GEM-T, Glen Mills Inc, Clifton, NJ) at inlet and outlet pressures of 60 and 40 psi, respectively. The powder was fed into the mill with a vibrating spatula. The product was collected from the mill's cyclone and collection jar. A portion of dried DF was also sieved with mesh sizes of 45, 75, 125, 150, 180, and 300 (Model No. SS-5, Gilson Company Inc, Worthington, OH). The sieved fractions of 45 μm to 75 μm and 75μm to 125 μm were used.

Volume diameters of the fluorescein powders were obtained by laser diffraction (HELOS Particle Size Analysis H0838, Sympatec GmbH, Germany) following shear dispersion (Rodos, Sympatec GmbH, Germany) with a pressure drop of 3.0 bar so that the particles could be broken down to the primary particle size. These volume diameters were converted to calculated aerodynamic diameters, Dac, using the density of DF, 1.46 g/mL [11]. The fractions of the fluorescein, jet milled, 45 μm to 75 μm, and 75 μm to 125 μm were blended with bulk lactose monohydrate (Mallinckrodt Inc, Paris, KY; density = 1.52 g/mL [12]) using a Turbula shaker-mixer (Model T2C, GlenMills, Inc, Clifton, NJ) to form 1% blends. The lactose-particle size distribution had a median aerodynamic diameter (Aerosizer, TSI, Minneapolis, MN) of 40.1 μm with a geometric standard deviation (GSD) of 1.63.

An Andersen MkII nonviable impactor was used to study the dispersion and flow of the particles. The collection plates were coated with 1% silicon oil (Fisher Scientific, Fair Lawn, NJ) in hexane (Sigma-Aldrich, St Louis, MO) before each experiment. Glass fiber filters with a pore size of 0.22 μm (Graseby Andersen, Smyrna, GA) were used below the last stage of the impactor. Gelatin capsules (size 3, Eli Lilly and Co, Indianapolis, IN) were filled with 20 mg of a blend (ie, 200 μg of fluorescein). These blends were then dispersed from a Rotahaler (GlaxoWellcome, Research Triangle Park, NC). A vacuum pump was used to draw air through the impactor at 60 L/min. Following actuation of the inhaler, sampling was continued for 10 seconds.

Three coating procedures for the preseparator were evaluated in addition to the 3 different blends studied. The preseparator was either untreated, its floor coated with 1% silicon oil in hexane, or treated with 10 mL of phosphate buffer (pH 7.4). The preseparator was divided into 4 regions: 1) the connection between the throat and the preseparator

(1P), 2) the floor of the preseparator (2P), 3) the side walls of the preseparator (3P), and 4) the inner and outer walls of the 3 orifices of the preseparator and the underside of the preseparator (4P) (Figure 4). Triplicate studies were performed for each blend with each of the different preseparator coatings. The relative humidity and temperature were recorded before each impaction experiment. A phosphate buffer of pH 7.4 was used to wash each of the preselected regions of the preseparator, the stages, the collection plates, and the filter. Ultraviolet spectrophotometry (Model UV160U, Shimadzu Scientific Instruments, Columbia, MD) was used to detect fluorescein with an absorbance maximum wavelength of 490 nm.

The inertial impaction data were used to determine the emitted doses and the fine particle fractions. The emitted dose was calculated as the percentage of the fluorescein escaping the inhaler, and the fine particle fraction was taken as the percentage of particles below 4.0 μm (ie, the particles deposited on stage 2 and below in the impactor). In addition, the nonballistic fraction [13] was calculated as the percentage of particles that deposited on the first collection plate (C-1) of those particles that entered the stages of the impactor. The impaction data were also used to determine the mass median aerodynamic diameters (MMAD) and GSD of the particle size distributions. Statistical differences between the different coating procedures were obtained using SigmaStat v. 1.0 (Jandel Scientific, San Rafael, CA) for the 3 particle-size ranges based on one-way analysis of variance (ANOVA).

RESULTS

The simple theoretical model of the preseparator shows the highest air velocity is likely to be at the openings to the exit orifice (Figure 5a). This high velocity is caused by the narrowing of the space through which the air must travel. The low-velocity regions appear to be near the center of the floor (A), above the orifice (B), and after exiting the orifice (C). According to the streamline plot of the preseparator (Figure 5b), these are also areas of air recirculation.

The velocity of the air through the top 3 stages of the impactor increases as the air travels around the outer edges of the collection plates and is highest through the inner orifices of each stage (Figure 5c). The streamline plot (Figure 5d) shows air recirculation near the outer walls of each stage and between the orifices above the collection plates. Although there are limitations to this model because the flow from the preseparator is certain to affect the flow through the stages, the model is qualitatively useful in showing where the low-velocity and high-pressure regions exist.

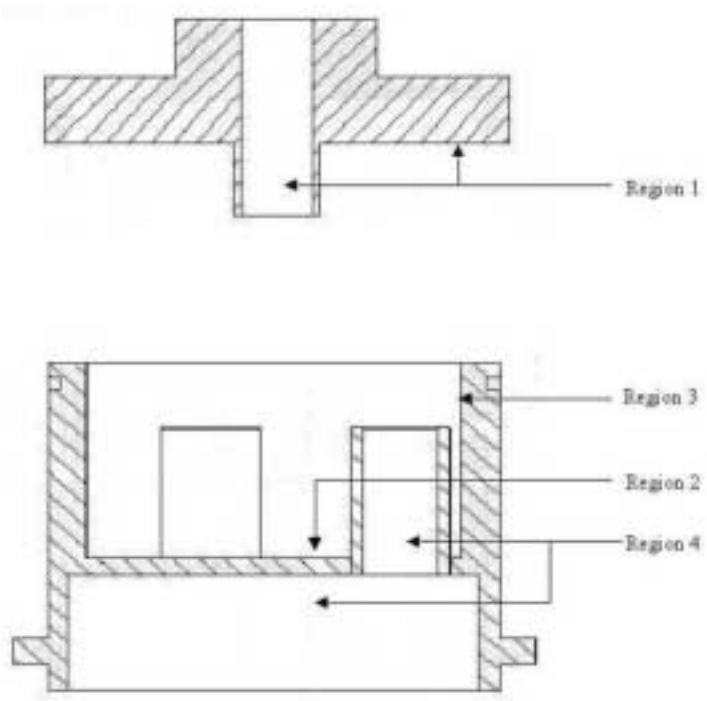

Figure 4. Preseparator and inlet jet regions for impaction runs.

Figure 5 (a.)

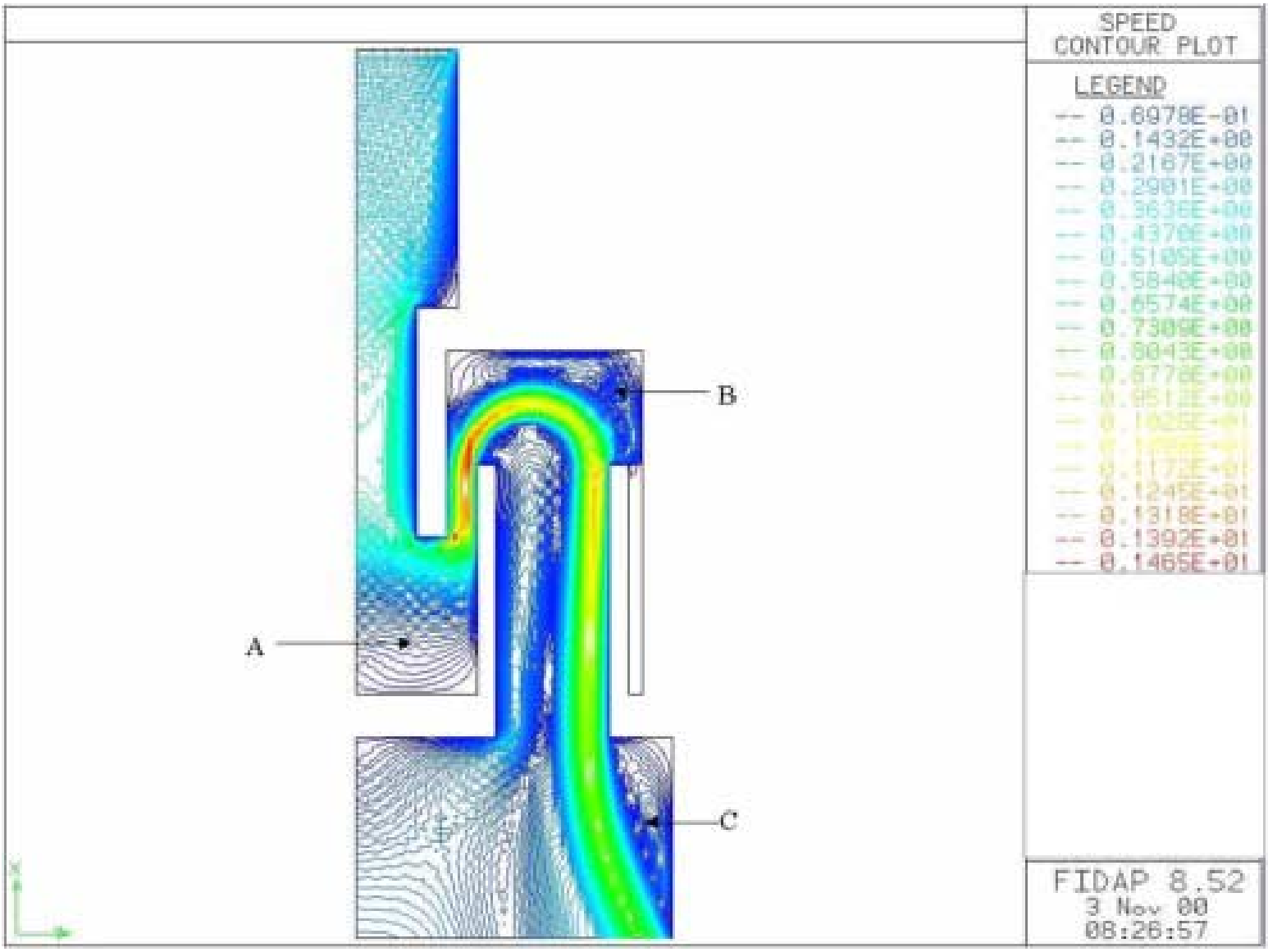
SPEED
CONTOUR PLOT
LEGEND
-- 0.6978E-01
-- 0.1432E+00
-- 0.2167E+00
-- 0.2901E+00
-- 0.3636E+00
-- 0.4370E+00
-- 0.5105E+00
-- 0.5840E+00
-- 0.6574E+00
-- 0.7309E+00
-- 0.8043E+00
-- 0.8778E+00
-- 0.9512E+00
-- 0.1025E+01
-- 0.1098E+01
-- 0.1172E+01
-- 0.1245E+01
-- 0.1318E+01
-- 0.1392E+01
-- 0.1465E+01
A
B
C
FIDAP 8.52
3 Nov 00
08:26:57

Figure 5 (b.)

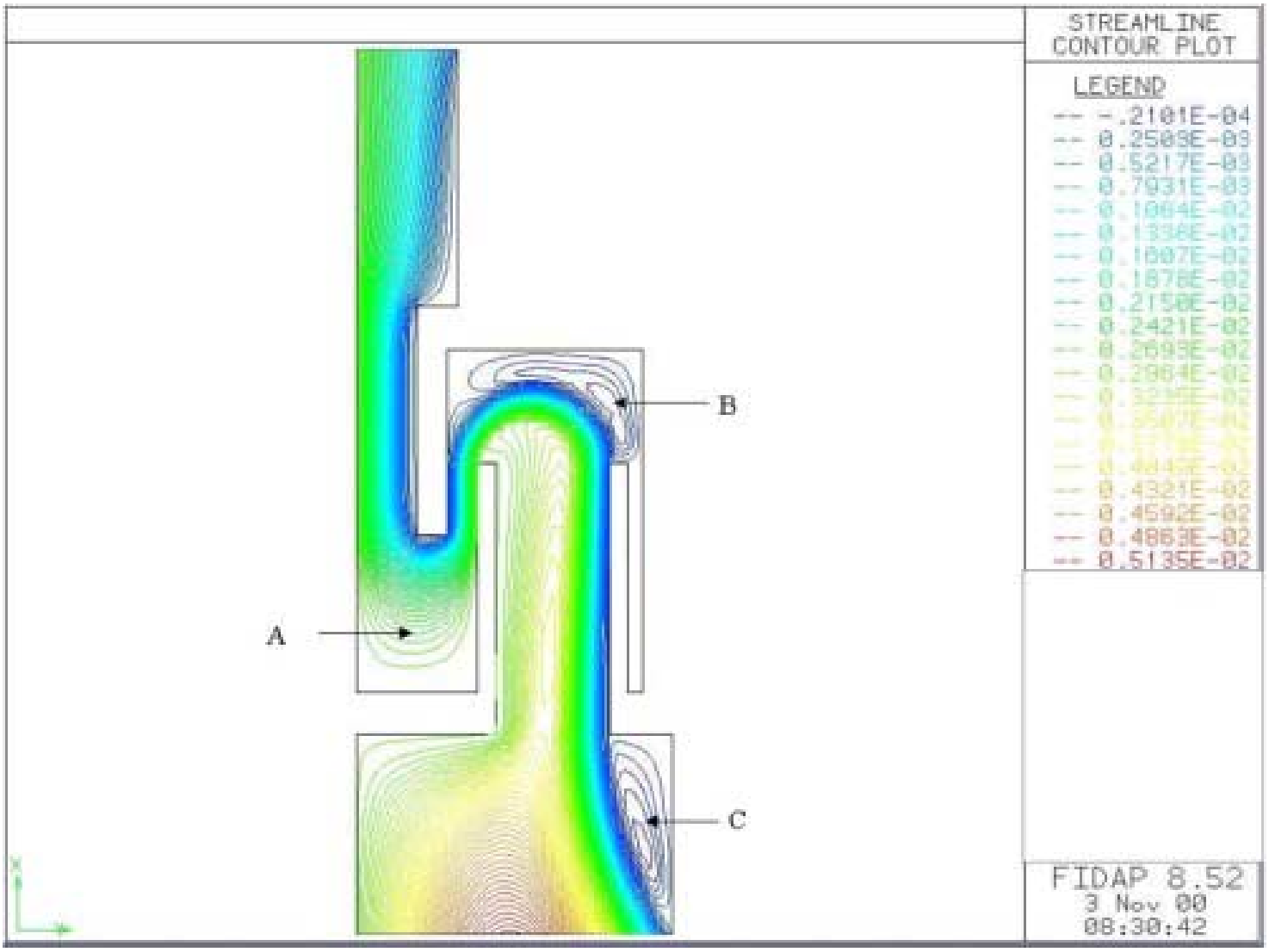
STREAMLINE
CONTOUR PLOT
LEGEND
-.2101E-04
0.2503E-03
0.5217E-03
0.7931E-03
0.1064E-02
0.1336E-02
0.1607E-02
0.1878E-02
0.2150E-02
0.2421E-02
0.2693E-02
0.2964E-02
0.4321E-02
0.4592E-02
0.4863E-02
0.5135E-02
FIDAP 8.52
3 Nov 00
08:30:42
A
B
C

Figure 5 (c.)

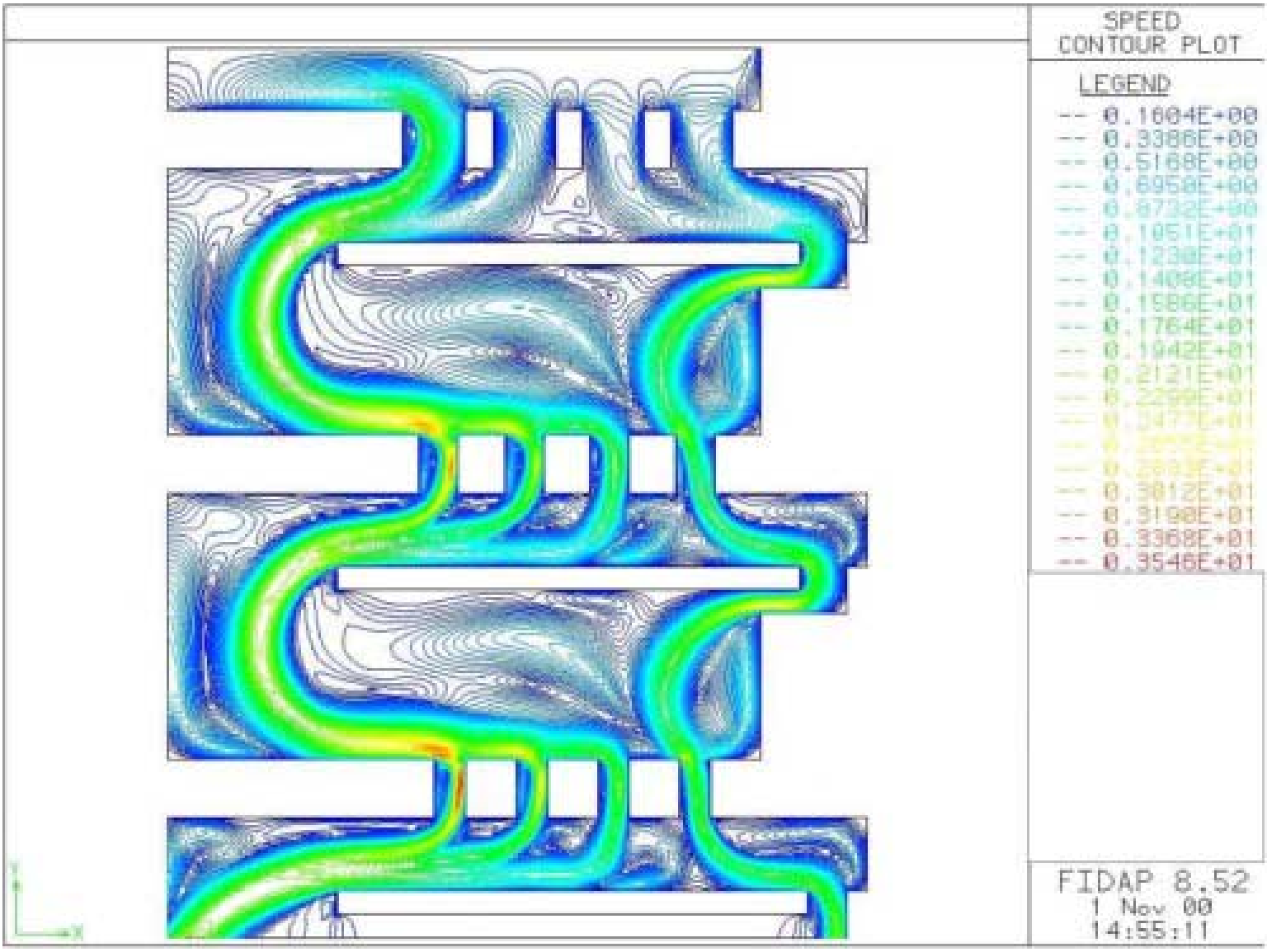
SPEED
CONTOUR PLOT
LEGEND
-- 0.1604E+00
-- 0.3386E+00
-- 0.5168E+00
-- 0.6950E+00
-- 0.8732E+00
-- 0.1051E+01
-- 0.1230E+01
-- 0.1408E+01
-- 0.1586E+01
-- 0.1764E+01
-- 0.1942E+01
-- 0.2121E+01
-- 0.3012E+01
-- 0.3190E+01
-- 0.3368E+01
-- 0.3546E+01
FIDAP 8.52
1 Nov 00
14:55:11

Figure 5 (d.)

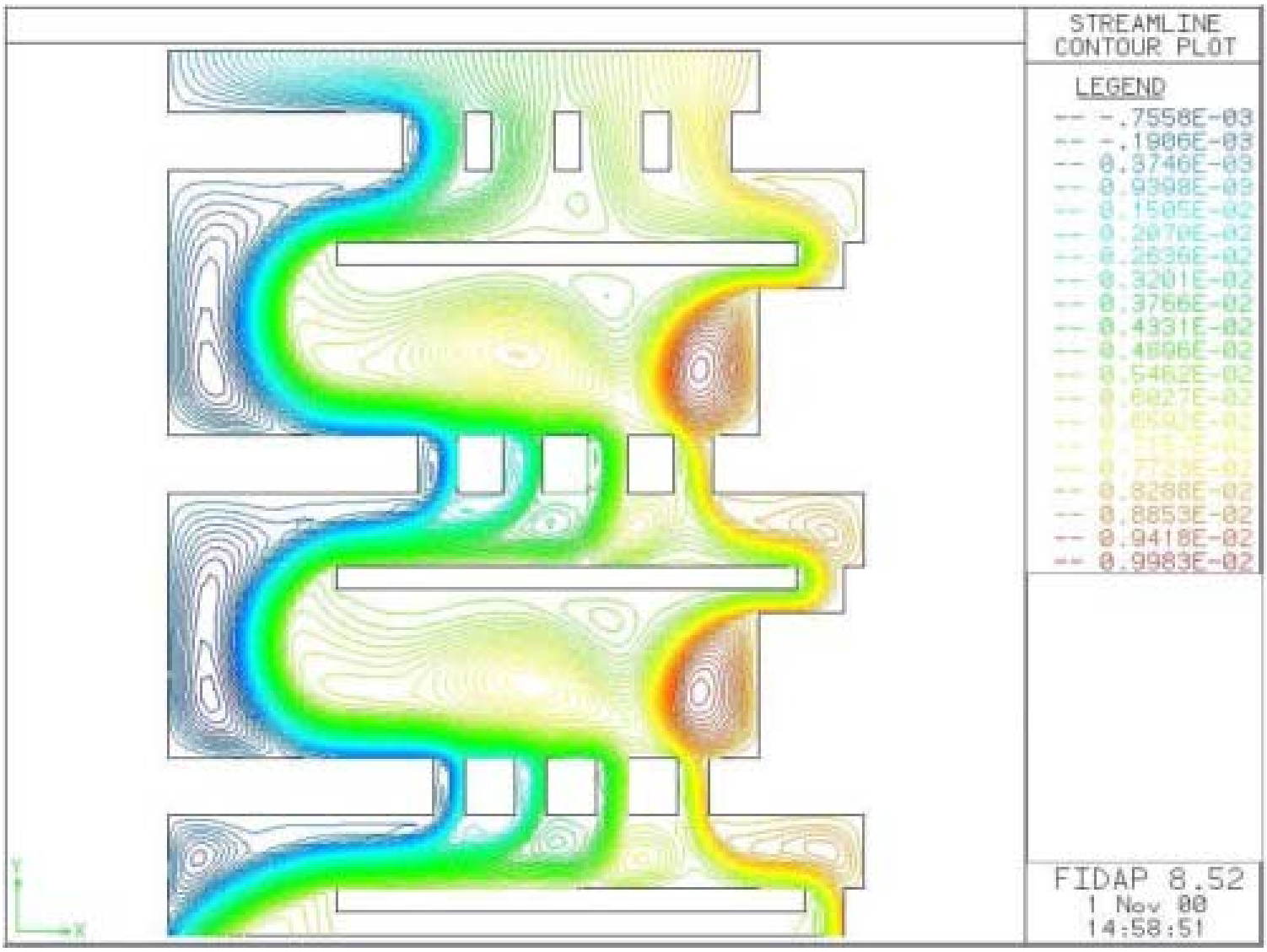

Figure 5. Models of preseparator and top 3 stages of the impactor (a) air speed through preseparator, (b) streamline plot of airflow through preseparator, (c) air speed through top 3 stages, (d) streamline plot of airflow through top 3 stages.

The convergence plots for the models of the preseparator and top 3 stages are illustrated in Figure 6. For the preseparator, convergence of the velocities, U and V, which correspond to v_r and v_z (equations 1 through 3), respectively, converge much more easily than does the solution for the pressure, P. For the top 3 stages, convergence of the velocities is also shown. The large difference between the number of iterations required for the preseparator compared to the stages results from using different techniques to solve for the 2 models.

The MMAD of the micronized particles and the sieved fractions determined by laser diffraction were below the cutoff diameter for the preseparator, 8.7 µm (6.7 µm for micronized particles), and above the cutoff diameter (34.9 µm for the 45-µm to 75-µm fraction and 24.4 µm for the 75-µm to 125-µm fractions), respectively. Sieving is less likely to break aggregates into primary particle sizes than is the shear disperser, which is used in laser diffraction particle size measurement. Consequently, the primary particle sizes estimated by laser diffraction were lower than those by sieving. This could also explain why the median calculated aerodynamic diameter, $MMAD_C$, for the 45-µm to 75-µm range is larger than for the 75-µm to 125-µm sieved fraction. The distributions for the fluorescein fractions are shown in Figure 7.

The results of the impaction experiments are shown in Figures 8, 9, and 10. The mass of particles in the 45-µm to 75-µm and 75-µm to 125-µm size ranges deposited on the collection plates was greater (58 ± 9 µg and 47 ± 2 µg, respectively) than the mass of micronized particles (34 ± 2 µg) in the presence of carrier lactose particles when the preseparator was untreated (Figure 8). When the preseparator was treated with silicon oil (Figure 9), the quantity of particles depositing on the collection plates was lower than without coating (17.5 ± 0.4 µg, 9 ± 4 µg and 6 ± 2 µg, respectively, for the micronized 45-µm to 75-µm and 75-µm to 125-µm size ranges). When the preseparator was filled with 10 mL of phosphate buffer (Figure 10), fewer large particles (2.6 ± 0.5 µg and 2 ± 1 µg, respectively, for the 45-µm to 75-µm and 75-µm to 125-µm size ranges) deposited on the collection plates. Most of the particles deposited in the coated area (region 2) when the preseparator was treated.

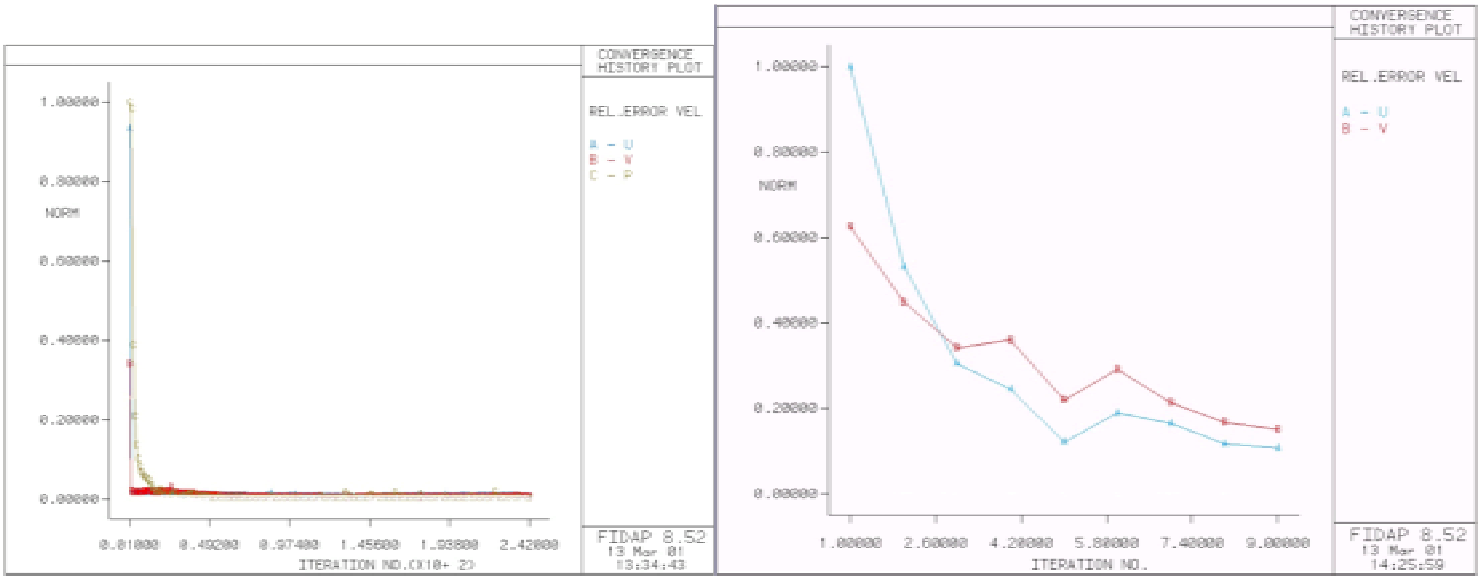

(a.) (b.)

Figure 6. Convergence of the velocities and pressure in the solution for (a) the preseparator and (b) the top 3 stages.

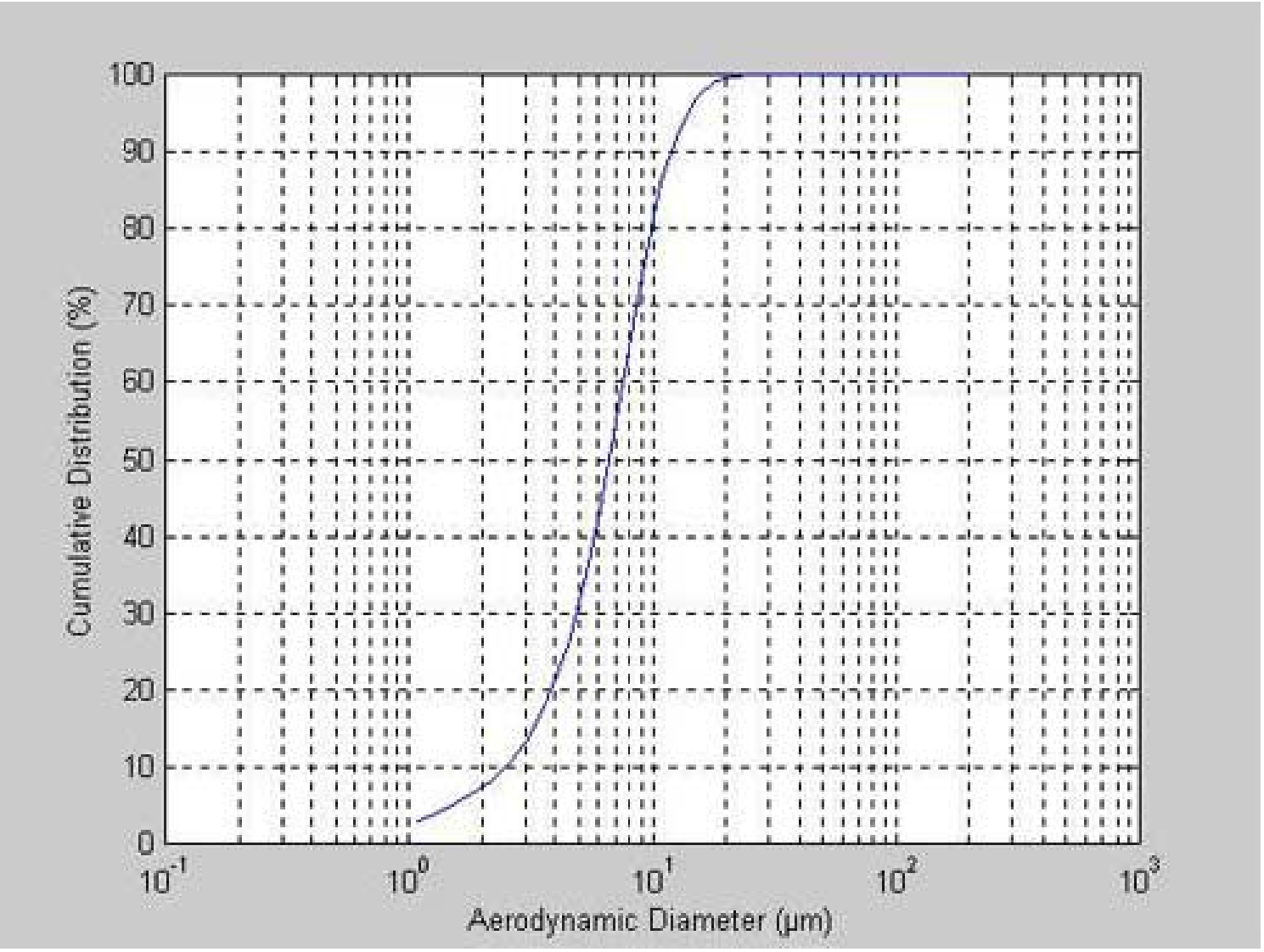
Cumulative Distribution (%)
100
90
80
70
60
50
40
30
20
10
0
10^{-1}
10^{0}
10^{1}
10^{2}
10^{3}
Aerodynamic Diameter (µm)

Figure 7 (a)

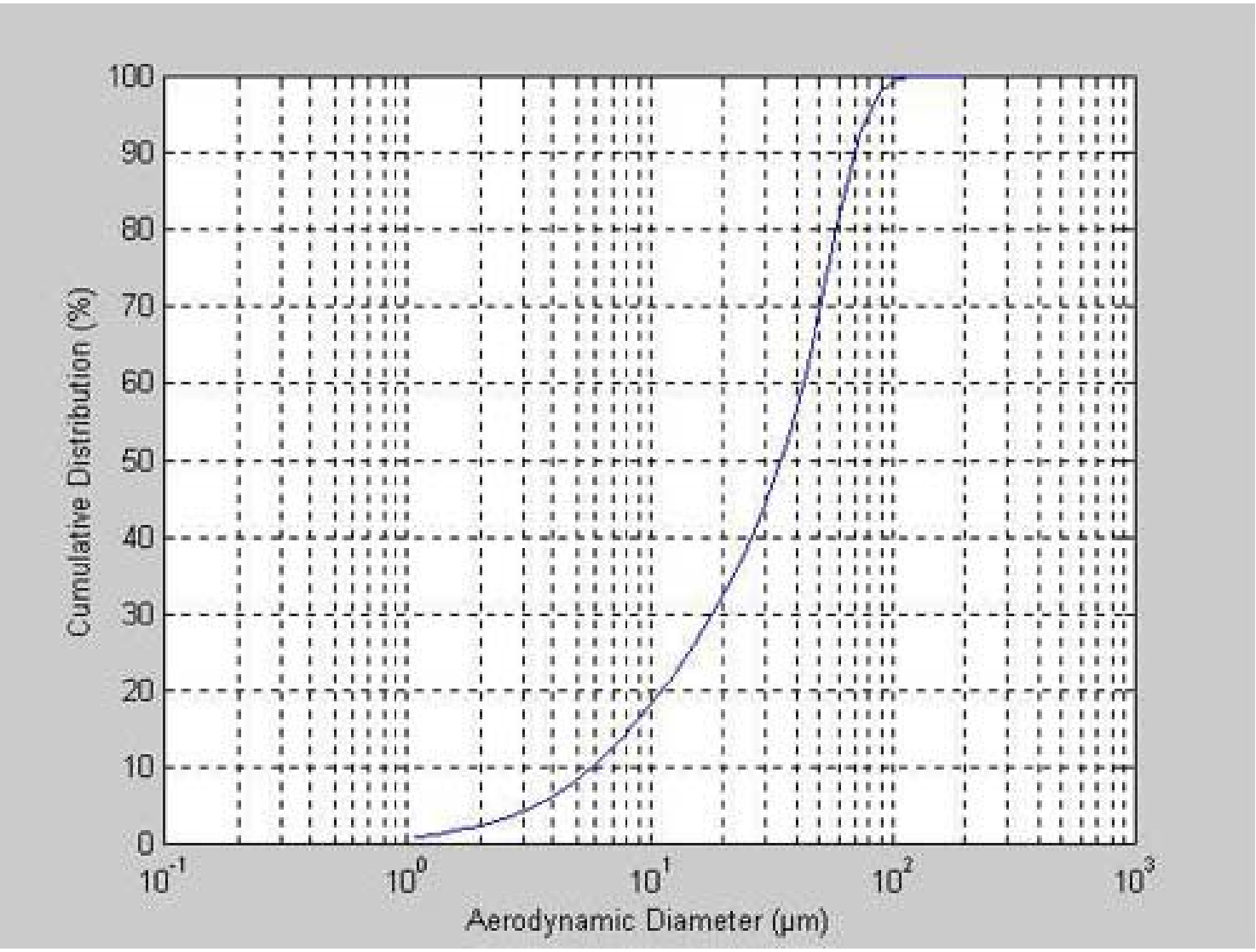
Cumulative Distribution (%)
100
90
80
70
60
50
40
30
20
10
0
10^{-1}
10^{0}
10^{1}
10^{2}
10^{3}
Aerodynamic Diameter (μm)

Figure 7 (b)

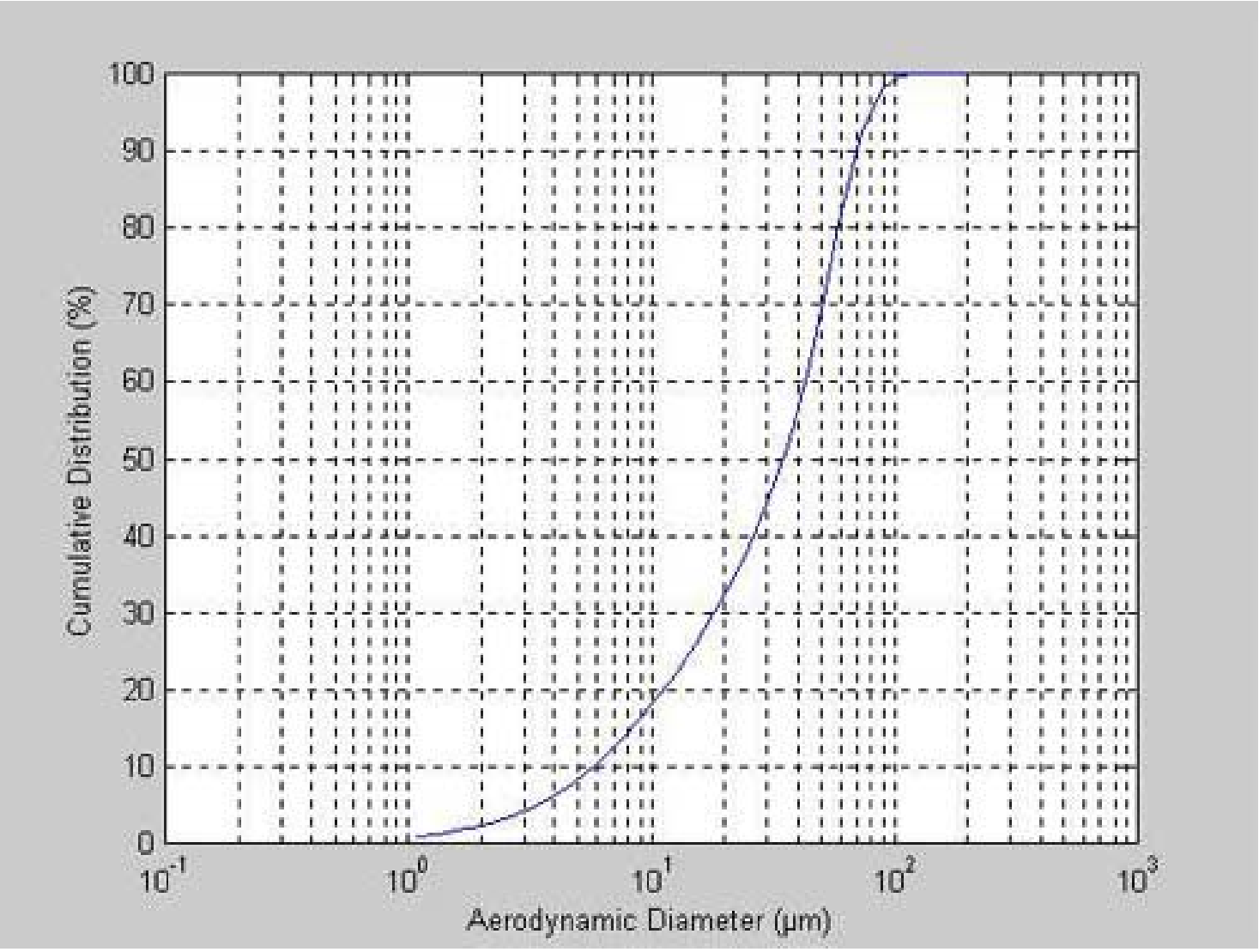

Figure 7 (c)

Figure 7. Aerodynamic diameter, Dac, distributions obtained by laser diffraction for (a) micronized particles, (b) 45-mm to 75-mm sieved fraction, and (c) 75-mm to 125-mm sieved fraction.

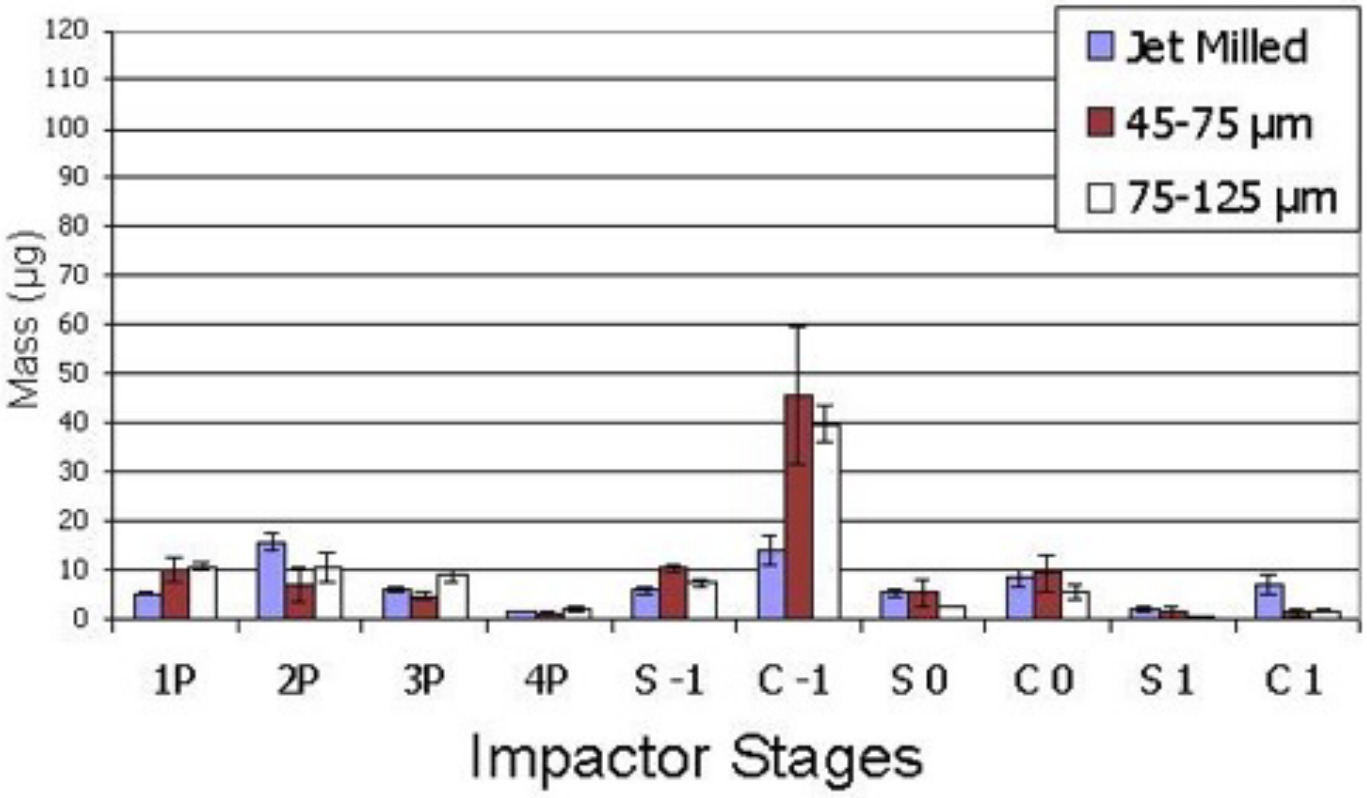

Figure 8. Cascade impaction samples from DF blends with the micronized, 45-µm to 75-µm and 75-µm to 125µm particles for the uncoated preseparator (1P, 2P, 3P, 4P), the top 3 stages (S-1, S0, S1), and the top 3 collection plates (C-1, C0, C1)

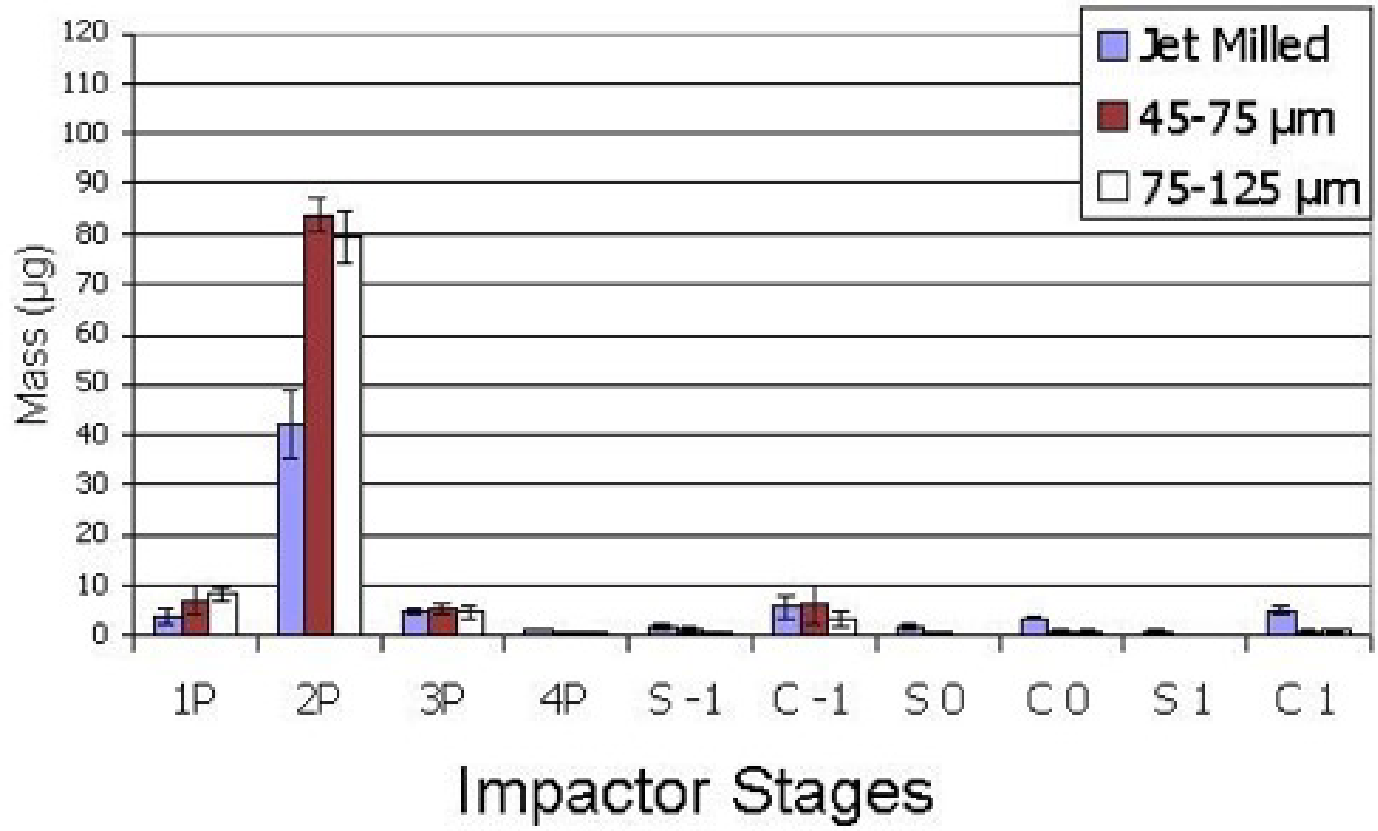

.

Figure 9. Cascade impaction samples from DF blends with the micronized, 45-µm to 75-µm and 75-µm to 125-µm particles for preseparator (1P, 2P, 3P, 4P) coated with 1% silicon oil in hexane, the top 3 stages (S-1, S0, S1), and the top 3 collection plates (C-1, C0, C1)

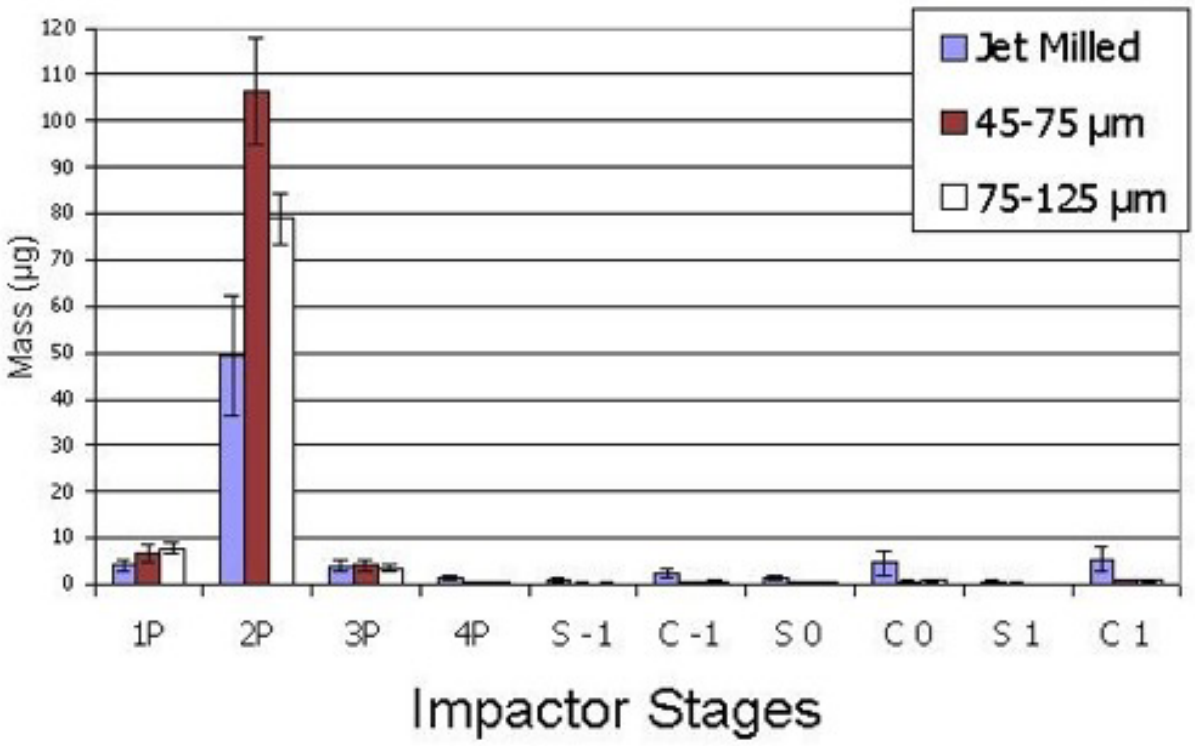

Figure 10. Cascade impaction samples from DF blends with the micronized, 45-µm to 75-µm and 75-µm to 125-µm particles for the preseparator (1P, 2P, 3P, 4P) filled with 10 mL of phosphate buffer (pH 7.4), the top 3 stages (S-1, S0, S1), and the top 3 collection plates (C-1, C0, C1).

Table 1 shows the emitted doses, fine particle fractions, and nonballistic fractions (NBF) for a variety of powders sampled under different preseparator conditions. Table 2 shows the comparisons based on ANOVA where *P* values less than 0.05 indicate statistical differences.

Table 1. Emitted Doses and Fine Particle Fractions (n = 3)

Preseparator Treatment	Powder	ED (%) Mean ± SD	FPF (%) Mean ± SD	NBF (%) Mean ± SD
Untreated	Micronized fluorescein	53 ± 6	5 ± 2	41 ± 11
	Fluorescein 45-75 µm	59 ± 9	1.5 ± 0.4	78 ± 12
	Fluorescein 75-125 µm	60 ± 4	0.9 ± 0.2	83 ± 5
Silicon Oil	Micronized fluorescein	47 ± 5	3 ± 1	33 ± 13
	Fluorescein 45-75 µm	56 ± 2	1.0 ± 0.3	65 ± 15
	Fluorescein 75-125 µm	63 ± 8	1.0 ± 0.4	53 ± 8
Buffer	Micronized fluorescein	52 ± 16	2 ± 1	17 ± 4
	Fluorescein 45-75 µm	70 ± 4	0.6 ± 0.2	19 ± 4
	Fluorescein 75-125 µm	57 ± 3	0.2 ± 0.1	25 ± 6

Note: ED indicates emitted doses; FPF, fine particle fractions; NBF, nonballistic fractions; SD, standard deviation.

Table 2. Statistical Differences between the Emitted Doses, Fine Particle Fractions, and Nonballistic Fractions

	Untreated vs Buffer			Untreated vs Silicon Oil			Silicon Oil vs Buffer		
	ED	FPF	NBF	ED	FPF	NBF	ED	FPF	NBF
Micronized	N	N	N	N	N	N	N	N	N
45-75 µm	S	S	S	N	N	N	S	S	S
75-125 µm	N	N	S	N	N	S	N	N	S

Note: ED indicates emitted doses; FPF, fine particle fractions; NBF, nonballistic fractions; S, statistical difference, $P < 0.05$; N, no statistical difference.

Table 3 shows the MMADs and GSDs of the aerodynamic particle size distributions.

Table 3. Mass Median Aerodynamic Diameters (MMAD) and Geometric Standard Deviations (GSD) of the Particle Size Distributions (n = 3)

Preseparator Treatment	Powder	MMAD (μm) Mean ± SD	GSD Mean ± SD
Untreated	Micronized fluorescein	7.0 ± 0.4	1.40 ± 0.20
	Fluorescein 45-75 μm	9.0 ± 1.0	1.31 ± 0.03
	Fluorescein 75-125 μm	11.2 ± 0.9	1.36 ± 0.02
Silicon Oil	Micronized fluorescein	6.3 ± 0.6	1.29 ± 0.03
	Fluorescein 45-75 μm	11.0 ± 2.0	1.38 ± 0.07
	Fluorescein 75-125 μm	9.0 ± 0.4	1.31 ± 0.02
Buffer	Micronized Fluorescein	6.3 ± 0.3	1.24 ± 0.02
	Fluorescein 45-75 μm	6.2 ± 0.9	1.20 ± 0.05
	Fluorescein 75-125 μm	7.1 ± 0.1	1.24 ± 0.01

Note: SD indicates standard deviation.

Table 4 shows the statistical differences between the MMADs and GSDs for the different preseparator coatings.

Table 4. Statistical Differences between Median Aerodynamic Diameters (MMAD) and Geometric Standard Deviations (GSD)

	Untreated vs. Buffer		Untreated vs. Silicon Oil		Silicon Oil vs. Buffer	
	MMAD	GSD	MMAD	GSD	MMAD	GSD
Micronized	N	N	N	N	N	N
45-75 μm	S	S	N	N	S	S
75-125 μm	S	S	S	S	S	S

Note: S indicates statistical difference, $P < 0.05$; N, no statistical difference.

DISCUSSION

Fluid dynamic models have been used to study flow profiles through different impactors and to indicate the locations of particle deposition; however, there are no published studies evaluating preseparator performance in the Andersen 8-stage sampler. Practically, coating has been recommended to decrease the number of particles larger than 8.7 μm in aerodynamic diameter from traveling past the preseparator and entering the calibrated stages of the impactor when operated at 60 L/min.

The simple models of the preseparator and the top 3 stages of the impactor qualitatively indicate the most likely particle deposition sites. These areas are primarily where the velocity of the air is low, whereas the pressure is high. It is likely that most particles will deposit on the center of the floor of the preseparator (Figure 5a), region 2. This is fortunate, because undoubtedly this is the intended outcome. However, there are other regions in the preseparator where particles may also deposit. For example, there is a low-velocity region above the entry orifices. Deposition in this area would mean greater wall losses and would not be desirable. The model of the upper stages shows that the areas of low velocity, high pressure, and particle deposition are on the centers of the stages where no orifices are present (Figure 5c). In addition, the interference between adjacent jets can cause decreased sharpness of the cutoff diameters of these stages. While the models presented in this work are based on several limiting assumptions that reduce their accuracy and constrain their interpretation, they do provide indications of high-pressure and low-velocity regions, which allowed sample site selection for the experimental studies.

The extent to which coating the preseparator influences the particle size determination with the impactor is dependent on the degree of coating. In the absence of coating, there is limited particle deposition in the preseparator for any particle size. Particles that impact on the floor of the preseparator are subject to bounce and re-entrainment. Coating the floor of the preseparator with a substance such as silicon oil provides an adhesive surface, preventing bounce and re-entrainment. In the absence of coating, particles in the 45-μm to 75-μm and 75-μm to 125-μm range deposited on the collection plates at the calibrated stages of the impactor (Figure 8). The quantity of particles in these size ranges that reached the stages and plates decreased when silicon oil was used for coating (Figure 9). The mass of particles reaching the first collection plate (P-1) was smaller than that for silicon oil, when the 10 mL of buffer was used for coating (Figure 10). Therefore, it appears that the

size selectivity of the preseparator is dependent on the degree of coating.

There were statistical differences in the emitted dose, fine particle fraction, and NBF between the untreated and the silicon oil treated preseparator when compared to the preseparator containing buffer for the 45-μm to 75-μm size range. This particle size range exhibited the largest $MMAD_C$, according to the laser diffraction studies. For the 75-μm to 125-μm sieved fraction, statistical differences in the NBF were detected between preseparator coating treatments. This is indicative of the effect of preseparator treatment on the mass of particles depositing on the entry stage (S-1). For the micronized DF particles, no statistical differences were observed between treatments. In general, differences between treatments resulted from the buffer being a more substantial collection medium in the preseparator.

The estimated MMAD decreased as the level of coating increased, since a smaller quantity of large particles entered the stages of the impactor. For the particles with an $MMAD_C$ above the cutoff diameter for the preseparator, 8.7 μm, the effect of the coating on the estimated MMAD was more significant than for particles with an $MMAD_C$ below the cutoff diameter. This is a result of the proportion of particles below 8.7 μm being significantly smaller when the mean diameter of the particle size distribution is above 8.7 μm. Therefore, there is an inverse relationship between the quantity of particles smaller than 5 μm entering the impactor and the extent of coating on the estimated MMAD. In some situations, depending on the composition and structure of particles used and their size, coating with silicon oil may be sufficient to prevent the particles greater than 8.7 μm from reaching the stages or the plates. However, in other cases, it may be necessary to use a more substantial collection medium. The coating of the preseparator has a significant effect on the resulting aerodynamic particle size distribution, particularly when large particles are present.

The aggregation of particles may play a critical role in using the impactor to study particle dispersion. Small particles, such as the micronized DF, may not disperse well and, consequently, become aggregated. When these aggregates impact on an uncoated preseparator, they may deaggregate and enter the impactor; however, if the aggregates impact in a medium on the preseparator's floor, deaggregation will not occur. When small particles are attached to large carrier particles, such as lactose, particle detachment occurs on impact with the preseparator, allowing a greater proportion of the small particles to enter the impactor than would enter from the dry powder inhaler alone. Because the deaggregation is prevented by a coating procedure, the treated preseparator more accurately represents the particle sizes that are aerodynamically capable of entering the impactor. In addition, this is a more accurate representation of the aerosol that would be delivered therapeutically. These studies have been performed using the Rotahaler, a device with poor dispersibility. It is important to recognize that not all dry powder inhalers would be sampled as inefficiently or unreproducibly.

The quantity of powder in the device before the impaction should be equivalent to the sum of that remaining in the device and that collected in the impactor. Wall losses are known to occur in the stages of the impactor. However, the nature and extent of wall losses in the preseparator of an impactor have not previously been evaluated. This study shows that the wall losses in regions 1, 3, or 4 of the preseparator for the Andersen impactor are less than 10% of the emitted doses. Particle deposition on regions 1, 3, and 4 with different coating procedures does not vary statistically. It is of great importance to know that the wall losses in these regions are small and are particle size independent. However, particles are collected in region 2 of the preseparator when coating is performed; this is indicated by the higher particle deposition of micronized particles (< 8.7 μm) in region 2 when coating is performed (Figures 9 and 10). Therefore, the coated surface of the preseparator accounts for most of the particle deposition in the preseparator. This is desirable because the coated surface prevents the

deaggregation of small particles and more accurately represents the particles aerodynamically capable of entering the impactor and ultimately, by inference, of delivering drug to the lungs.

The phenomenon of preseparator efficiency in sampling aerosol particles might be more comprehensively studied using monodisperse aerosols. The present studies indicate the need for such a thorough evaluation.

CONCLUSIONS

Theoretical models have been used to predict where particle deposition was most likely to occur in the Andersen impactor. These areas have low velocity airflow and high local pressure. Deposition seemed most likely to occur in the center of the floor of the preseparator, as would be expected. In the upper impactor stages, this deposition appeared to occur at the center of the stages where no orifices are present.

The experimental work performed in this study showed that the particle size determination with the impactor was dependent on the nature of coating of the preseparator. Coating was useful in preventing bounce and re-entrainment to the stages and collection plates of the impactor of particles greater than 8.7 μm in aerodynamic diameter. Coating the floor of the preseparator did not significantly affect the deposition in other regions of the preseparator. The coating prevented deaggregation of particles, which affected the estimates of particle size as these deaggregated particles could enter the stages of the impactor.

ACKNOWLEDGEMENTS

The authors would like to thank Jonathan Masters and Dr Carol Lucas of the Biomedical Engineering Department at the University of North Carolina at Chapel Hill for their assistance with the finite element analysis. We would also like to thank the North Carolina Supercomputing Center for use of their facilities. This work was supported by NIH Grant # HL55789. We would like to thank the reviewers of this article for the images provided of the preseparator.

REFERENCES

1. May KR. The cascade impactor: an instrument for sampling coarse aerosols. J Sci Instr. 1945;22:187-195.

2. Vaughan NP. The andersen impactor: calibration, wall losses and numerical simulation. J Aer Sci. 1989;20(1):67-90.

3. Swanson PD, Kushleika J, Checkoway H, et al. Numerical analysis of motion and deposition of particles in cascade impactors. Int J Pharm. 1996;142:33-51.

4. Marple VA. A fundamental study of inertial impactors [dissertation]. University of Minnesota, 1970.

5. Operating manual for Andersen 2000 ambient particle sizing sampler. Atlanta, Ga: Andersen 2000 Inc.; 1977.

6. US Pharmacopoeia. USP 24 Aerosols, Metered-Dose Inhalers, and Dry Powder Inhalers. Rockville, MD: USP; 1999.

7. British Pharmacopoeia. Preparations for Inhalation.Vol. II. London, England: The Stationary Office; 1999.

8. Rader DJ, Marple VA. Effect of ultra-stokesian drag and particle interception on impaction characteristics. Aer Sci Tech. 1984;4:141-156.

9. Welty JR, Wicks CE, Wilson RE. Fundamentals of Momentum, Heat, and Mass Transfer. 3rd ed. New York: John Wiley & Sons; 1984:732-733.

10. Greenspan B. A response to the stimuli to the revision process article: verification of operating the andersen cascade impactor at different flow rates. Pharm Forum. 1996;22(6):3288-3292.

11. Hickey AJ, Jackson GV, Fildes FJT. Preparation and characterization of disodium fluorescein powders in association with lauric and capric acids. J Pharm Sci. 1988;77(9):804-809.

12. American Pharmaceutical Association.Handbook of Pharmaceutical Excipients. Washington, DC: American Pharmaceutical Association; 1986.

13. Thiel CG. Can in vitro particle size measurements be used to predict pulmonary deposition of aerosol from inhalers? J Aer Med. 1998;9(Suppl. 1):S43-S52.